# Inverse problems in sun photometry for integral aerosol distributions. II. Division into submicron and coarse fractions

**V.V. Veretennikov**

*Institute of Atmospheric Optics,*
*Siberian Branch of the Russian Academy of Sciences, Tomsk*

Received October 3, 2005

The numerical results on modeling the reconstruction of aerosol microstructure parameters divided into particle size fractions are presented. Solution of the inverse problem is based on the description of aerosol microstructure using integral distributions. In the case of submicron and coarse aerosol fractions, the developed method allows an estimate of the volume packing factor to be obtained with a 10% error; the average particle radius can be reconstructed accurate to 0.02–0.06 μm.

## Introduction

This paper is the second part of the study (see Ref. 1), in which some aspects of the technique of using integral aerosol distributions in solving the inverse problems in sun photometry have been considered. It was shown that passing from differential particle size distributions to integral distributions in describing the aerosol microstructure provides for obtaining a stable solution to the inverse problem by minimization of the functional of discrepancy under natural limitations of the class of admissible solutions (non-negativity, monotonicity, boundedness). Having known the integral size distribution, one can easily pass to more conventional parameters characterizing the properties of aerosol microstructure, such as number density, mean particle size, distribution width, etc.

Although the aforementioned parameters can be sufficient for solving many problems, it is yet interesting to obtain more detailed data on the state of microstructure from the data on the integral aerosol distributions. First, this relates to determination of the parameters of aerosol microstructure in the local ranges of the range of definition. Such a problem appears, for example, in the case when aerosol has several size fractions, the properties of which can change independently. Then it is important to observe not only the microphysical state of the entire ensemble of particles, but the parameters of each of its fractions.

The results obtained by numerical experiments on determination of the mean radius and the volume packing factor from the integral aerosol distributions retrieved from inversion of the extinction coefficient are presented in Ref. 1. The model of microstructure included only the submicron fraction for which the model of the haze H type was taken.[2] Analogous problem is considered in this paper for the model of aerosol comprising two fractions, the submicron and the coarse ones. The parameters of microstructure were retrieved in numerical experiments both for the medium as a whole and for the both of its fractions. The spectral dependences of the extinction coefficient were supplemented by measurement data on the scattering phase functions in the small-angle range and taken as input parameters for solving the inverse problem.

## 1. Optical and microstructure model of the scattering medium

As mentioned in the introduction, the model of the disperse medium comprising two aerosol fractions, submicron (s) and coarse (c) was used in the numerical experiment. The modified gamma-distribution with the parameters corresponding to the haze H model (Ref. 2) are taken for the model of submicron fraction, and analytical description of the coarse fraction is made using a wide lognormal distribution. The values of the mean radius $\bar{r}_s$ of the fractions are set at 0.25 and 1.23 μm, respectively.

The weights, with which the aforementioned fractions contribute to the total size distribution, can be varied to provide for a preset relative contribution $p = \varepsilon_c(\lambda^*)/\varepsilon(\lambda^*)$ of the coarse fraction to the extinction coefficient at some wavelength $\lambda^*$ under additional condition that $\varepsilon(\lambda^*) = 1$ km$^{-1}$ ($\lambda^* = 0.55$ μm). Selecting different values $p$ ($0 \le p \le 1$), one can obtain the shape of the modeled distribution in a wide range. Two extreme cases correspond to the situations, in which only one of the considered fractions is present, the submicron ($p = 0$) or the coarse one ($p = 1$). The case of $p = 0$ was considered in detail in the first part of this study.[1] Therefore, let us consider now the case $p > 0$.

Figure 1*a* shows the dependence of the size distribution of the particle geometric cross sections $s(r)$ at the value $p = 0.3$ (curve *3*), when the submicron fraction of particles prevailed in scattering of light in the visible range. The integral distribution $S_\downarrow(r) = \int_r^R s(r')\mathrm{d}r'$, shown below in Fig. 4 (curve *1*) just corresponds to this case. Figure 1*b*, in which the

0235-6880/06/04 266-07 $02.00 

dependences for $p = 0.5$ are shown, gives an idea about the changes occurring in the particle size spectrum with the increasing content of coarse fraction particles. It is seen from Fig. 1 that the submicron fraction practically disappears at $r > 0.7$ μm, and the coarse fraction becomes dominating.

The discrete set of the extinction coefficient values $\varepsilon(\lambda)$ in the wavelength range [0.31; 4.0] μm and the scattering phase functions in the angular range from 2 to 12° was calculated using the selected models of the microstructure. Then, after introducing the error, they served as the initial data for solving the inverse problem.

Figure 2 shows the calculated results on the spectral dependence of the extinction coefficient $\varepsilon(\lambda)$ (curve *3*) for the case of two-component model of the aerosol medium with the size distribution function of the particle geometric cross sections $s(r)$ shown in Fig. 1. The dependences $\varepsilon_s(\lambda)$ (curve *1*) and $\varepsilon_c(\lambda)$ (curve *2*) of s and c aerosol fractions are also shown in this figure. The complex refractive index $m = n - i\kappa$ was taken the same for both of the fractions and equals to $1.5 - i \cdot 0$ at all the wavelengths. The value $\varepsilon_c(\lambda)$ for the model shown in Fig. 2*a* at the wavelength of $\lambda = 0.55$ μm is 20% of the value of the total extinction coefficient $\varepsilon(\lambda)$. If moving to the right from this wavelength, the role of c fraction in the extinction of light continuously increases, and at $\lambda = 1.18$ μm it becomes prevalent. As is seen from Fig. 2*a*, variability of the function $\varepsilon(\lambda)$ in the wavelength range considered is caused mainly by the s aerosol fraction, for which the extinction coefficient $\varepsilon_s(\lambda)$ has maximum at the wavelength of $\lambda = 0.37$ μm and dramatically decreases at the wavelengths into the IR range. Extinction of light by particles of c fraction has more smooth spectral dependence with the maximum near $\lambda = 1.3$ μm, and then it gradually decreases by about two times at the long-wave edge of the wavelength range. Position of the maximum in the spectrum is close to the mean radius $\bar{r}_s$ of the c fraction particles.

Figure 2*b* shows how the ratio of the contributions coming from the aerosol fractions to the extinction of light changes with the parameter $p$ increasing up to 0.5. The peculiarity of this example is the fact that, starting from $\lambda = 0.55$ μm and longer, c fraction dominates throughout the rest part of the spectral range considered. Nevertheless, qualitatively, the spectral dependence of the light extinction characteristics of the s aerosol fraction is evident in the behavior of the total extinction coefficient $\varepsilon(\lambda)$ up to $\lambda = 1.3$ μm.

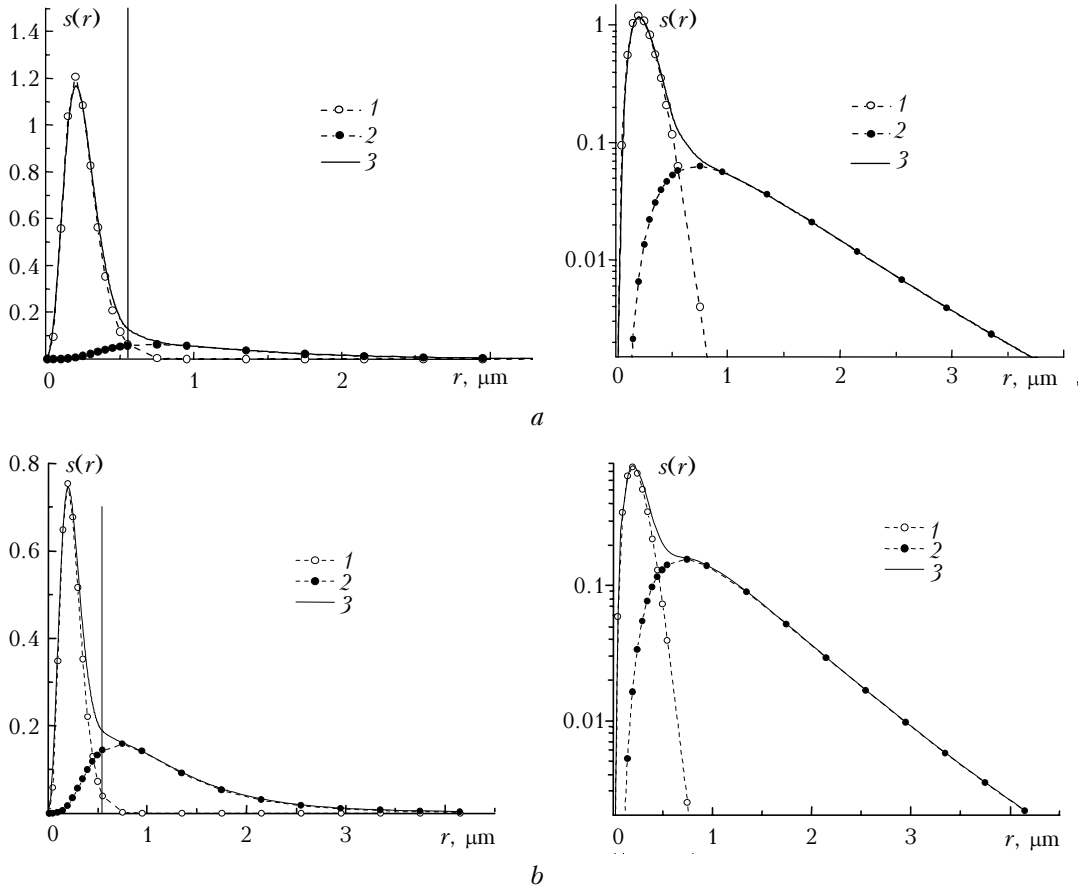


**Fig. 1.** Size distributions of submicron (*1*) and coarse (*2*) aerosol fractions and their weighted sum (*3*), $p = 0.2$ (*a*), 0.5 (*b*).

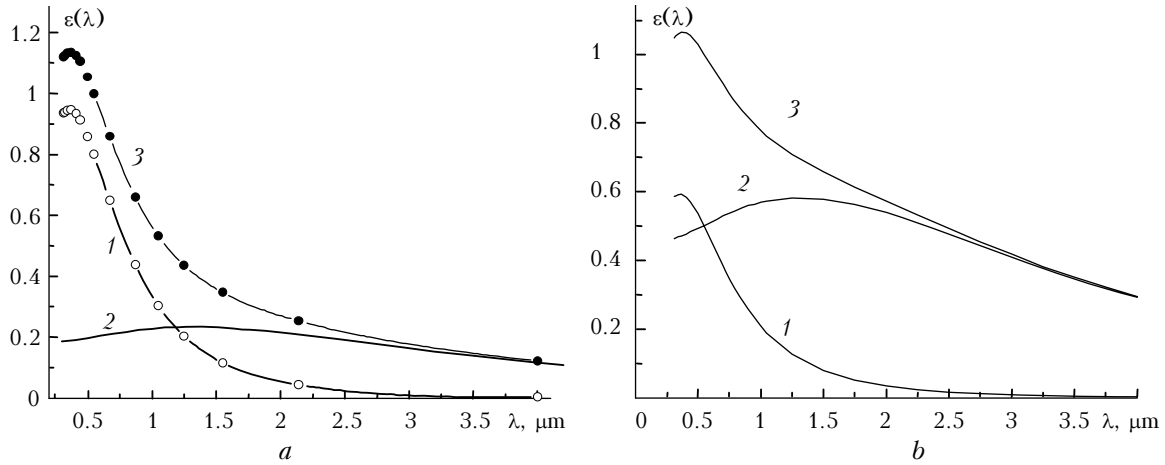


**Fig. 2.** Spectral behavior of the extinction coefficient ε(λ) for the aerosol model shown in Fig. 1: contributions of submicron (*1*) and coarse (*2*) aerosol fractions and their sum (*3*); $p = 0.2$ (*a*), 0.5 (*b*).

Let us now consider the effect of microstructure of a two-component model medium on the behavior of aureole scattering phase function. The behavior of the total scattering phase function μ(θ) and its components $\mu_s(\theta)$ and $\mu_c(\theta)$ at the wavelength of $\lambda = 0.55$ μm in the range of scattering angles $\theta = 2–12°$ at $p = 0.2$ is shown in Fig. 3*a*.

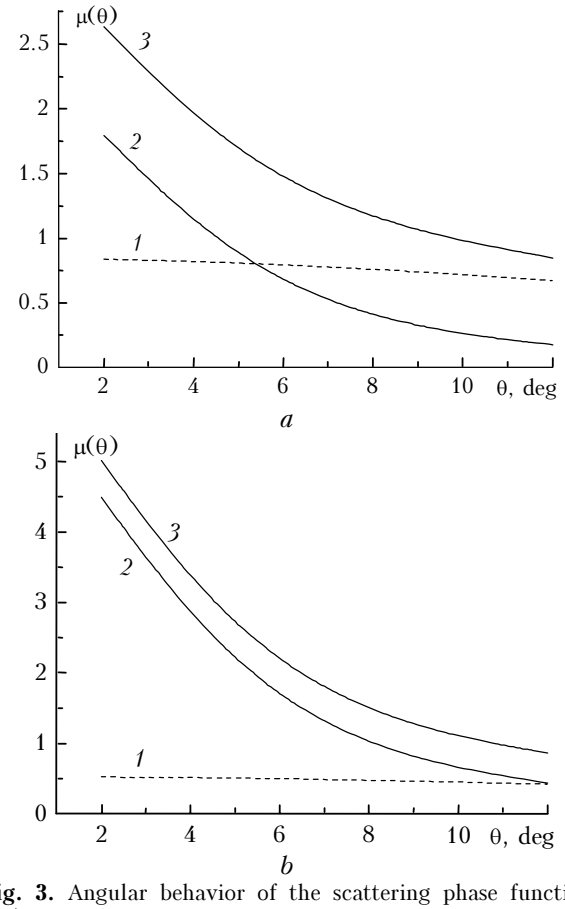


**Fig. 3.** Angular behavior of the scattering phase function μ(θ) at the wavelength $\lambda = 0.55$ μm for the aerosol model shown in Fig. 1: contributions of submicron (*1*) and coarse (*2*) aerosol fractions and their sum (*3*); $p = 0.2$ (*a*), 0.5 (*b*).

It is seen from Fig. 3*a* that the scattering phase function $\mu_s(\theta)$ in this angular range changes insignificantly thus demonstrating low information content of the measurements data in relation to the s aerosol fraction. At the same time, this fraction makes the main contribution to the scattering at the angles larger than 5.5°.

As the parameter $p$ increases, the role of s aerosol fraction in small-angle scattering decreases even stronger, and, as is seen, for example, from Fig. 3*b*, the contribution of c aerosol fraction becomes dominating at $p = 0.5$ throughout the entire range of scattering angles considered. On the whole, one should expect that measurements of the aureole scattering phase functions could be promising for diagnostics of the parameters of microstructure of only c aerosol fraction. This conclusion is also valid for other wavelengths.

*Simulation of the measurement errors.* In numerical experiments random errors were introduced into the $i$th measurement of the optical parameter $f_{0i}$ according to the following rule:

$$f_i = f_{0i}(1 + k_i\delta_i), \qquad (1)$$

where the coefficient $k_i = \varepsilon_{0,1}/\varepsilon_{0i}$ for spectral measurements $f_{0i} = \varepsilon_{0i}$ while for angular measurements $k_i = 1$ $f_{0i} = \mu_{0i}$; $\delta_i = \delta(2\eta_i - 1)$, δ determines the level of the relative error, and $\eta_i$ is the realization of a random value uniformly distributed over the interval [0, 1).

## 2. Simulation of the inverse problem for the extinction coefficient

The results of numerical experiments on solving the inverse problem for the light extinction coefficient for the case when submicron and coarse fractions of aerosol are present in its disperse composition (see Fig. 1) are discussed in this section.

In solving the inverse problem, the integral distribution $S_\downarrow(r)$ was retrieved using the algorithm

from Ref. 1. Then the total geometrical cross section of particles $S = S_{\downarrow}(0)$, the mean radius of particles $\bar{r}_s = S^{-1}\int_0^R S_{\downarrow}(r)\mathrm{d}r$, as well as the volume packing factor $V = (4/3)S\bar{r}_s$ were determined. As the medium in this case is formed by two size fractions of aerosol, it is also interesting to estimate the aforementioned parameters in the subintervals, where these fractions are mainly located. Based on the analysis of aerosol distributions shown in Fig. 1, the value $R^* = 0.55$ μm was taken as the boundary separating the two fractions. This boundary is shown by vertical line in Fig. 1. The integral distributions of individual fractions have the following form:

$$S_{\downarrow}^{(s)}(r) = \begin{cases} S_{\downarrow}(r) - S_{\downarrow}(R^*), & r \le R^*, \\ 0, & r > R^*, \end{cases} \quad (2)$$

$$S_{\downarrow}^{(c)}(r) = \begin{cases} S_{\downarrow}(R^*), & r \le R^*, \\ S_{\downarrow}(r), & r > R^* \end{cases} \quad (3)$$

for s and c fraction, respectively, and analogous parameters of microstructure of the fractions were calculated by the formulas

$$S^{(s)} = S - S_{\downarrow}(R^*), \quad S^{(c)} = S_{\downarrow}(R^*), \quad (4)$$

$$V^{(s)} = (4/3)\int_0^{R^*} S_{\downarrow}^{(s)}(r)\mathrm{d}r, \quad V^{(c)} = V - V^{(s)}, \quad (5)$$

$$\bar{r}_s^{(s)} = (3/4)V^{(s)}/S^{(s)}, \quad \bar{r}_s^{(c)} = (3/4)V^{(c)}/S^{(c)}. \quad (6)$$

## 2.1. Results obtained by the inversion at $p = 0.2$

The solutions of the inverse problem for the spectral dependences of the extinction coefficient ε(λ) at $p = 0.2$ (see Fig. 2*a*) with random error introduced in by Eq. (1) are shown in Fig. 4.

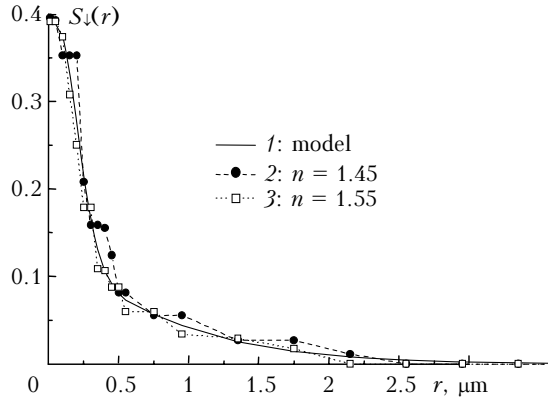


**Fig. 4.** Examples of inverting the spectral measurements into the extinction coefficient ε(λ): *1* is the model distribution $S_{\downarrow 0}(r)$ for $p = 0.2$; *2* and *3* are distributions $S_{\downarrow\delta}(r)$ retrieved at different values of the refractive index and measurement error $\delta = 0.1$.

As in the case with the only fraction at $p = 0$ (Ref. 1), in the considered example, the errors in setting the real and imaginary parts of the refractive index did not exceed 0.05 by the absolute value. As is seen from Fig. 4, all the retrieved solutions $S_{\downarrow\delta}(r)$ are located within the argument limits $r < 2.15$–$2.55$ μm. The contribution coming from particles with the sizes out of this range to the total cross section described by the exact distribution $S_{\downarrow 0}(r)$ does not exceed 1–2%.

The estimated integral parameters of the microstructure $V$ and $\bar{r}_s$ from the retrieved distributions $S_{\downarrow\delta}(r)$ are presented in Tables 1 and 2. The integral parameters of individual fractions $\bar{r}_s^{(s)}$ and $V^{(s)}$ and $\bar{r}_s^{(c)}$ and $V^{(c)}$ were calculated for the subranges [0; 0.55] μm and [0.55; 4.15] μm, respectively.

Table 1 contains the data on the volume packing factor retrieved with the fraction separation. The volume of particles of each fraction is approximately the same. High accuracy of determination of the total packing factor $V$ attracts one's attention as the error is about 0.5% at the known refractive index and increases up to 10% in the presence of errors in the refractive index. As to individual fractions, in general the packing factors $V^{(s)}$ and $V^{(c)}$ are retrieved worse i.e., the error reaches 10% already for known refractive index. The errors in setting the refractive index stronger affect the estimate of $V^{(c)}$ which increases up to 22% at $\kappa = 0.05$.

**Table 1. Retrieved values of the volume packing factor $V$ in the problem of inverting the spectral dependences ε(λ) at $p = 0.2$ and $\delta = 0.1$**

| Parameter | Exact data | $n$ = 1.5 | $n$ = 1.45 | $n$ = 1.55 | $\kappa$ = 0.05 |
|---|---|---|---|---|---|
| $V$ | 0.227 | 0.226 | 0.249 | 0.210 | 0.217 |
| $V^{(s)}$ | 0.102 | 0.112 | 0.108 | 0.105 | 0.119 |
| $V^{(c)}$ | 0.125 | 0.113 | 0.142 | 0.105 | 0.098 |

Table 2 has analogous structure and contains the data on the retrieved mean radii in the entire size range as a whole and with the fraction separation.

**Table 2. Retrieved values of the mean radii of the model distributions in the problem of inverting the spectral dependences ε(λ) at $p = 0.2$ and $\delta = 0.1$**

| Parameter, μm | Exact data | $n$ = 1.5 | $n$ = 1.45 | $n$ = 1.55 | $\kappa$ = 0.05 |
|---|---|---|---|---|---|
| $\bar{r}_s$ | 0.437 | 0.460 | 0.472 | 0.402 | 0.419 |
| $\bar{r}_s^{(s)}$ | 0.241 | 0.273 | 0.257 | 0.237 | 0.262 |
| $\bar{r}_s^{(c)}$ | 1.285 | 1.448 | 1.30 | 1.323 | 1.527 |

As in the case of retrieving the volume packing factor, the estimates of $\bar{r}_s$, which characterize the disperse composition as a whole, are more accurate here. The absolute error in determining the mean radius $\bar{r}_s$ is about 0.02 μm at the known refractive index and can increase up to 0.035 μm at $|\Delta n| = 0.05$. The error in determining $\bar{r}_s^{(s)}$ for particles of submicron range is a little bit greater and equals to

*

0.03 μm for $n = 1.5$. The absolute value of the error in determining the mean radius of particles of the coarse fraction $\bar{r}_s^{(c)}$ is greater. It is 0.16 μm at the known refractive index.

### 2.2. Results obtained by the inversion at $p = 0.5$

The distributions $S_{\downarrow\delta}(r)$ retrieved in the numerical experiment at a higher contribution of the coarse fraction ($p = 0.5$) are shown in Fig. 5. The other conditions of the numerical simulation are identical to the case of $p = 0.2$.

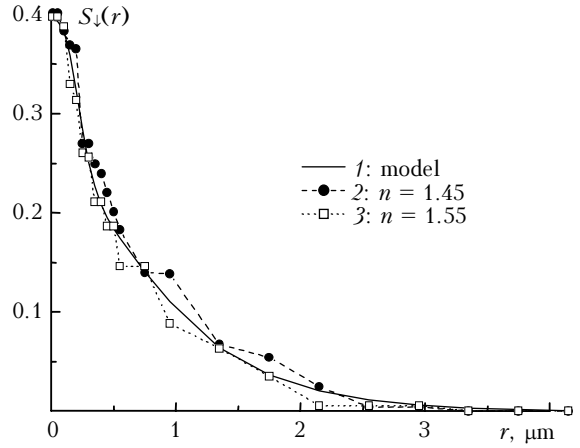


**Fig. 5.** Examples of inverting the spectral measurements into the extinction coefficient ε(λ): *1* is model distribution $S_{\downarrow 0}(r)$ for $p = 0.5$; *2* and *3* are distributions $S_{\downarrow\delta}(r)$, retrieved at different values of the refractive index and measurement error $\delta = 0.1$.

The corresponding estimates of the parameters of microstructure are presented in Tables 3 and 4. Let us note the main differences of the obtained results from those in the previous case. First, as is seen from Fig. 5, the upper boundary of the size range, where the retrieved microstructures are located, is shifted to the right being about 3.35–3.75 μm. The fraction of particles with the sizes out of this boundary is low in the model distribution $S_{\downarrow\delta}(r)$ as before, being no higher than 1% of the geometrical cross section.

**Table 3. Retrieved values of the volume packing factor $V$ in the problem of inverting the spectral dependences ε(λ) at $p = 0.5$ and $\delta = 0.1$**

| Parameter | Exact data | $n = 1.5$ | $n = 1.45$ | $n = 1.55$ | $\kappa = 0.05$ |
|---|---|---|---|---|---|
| $V$ | 0.382 | 0.367 | 0.412 | 0.351 | 0.359 |
| $V^{(s)}$ | 0.0758 | 0.0937 | 0.0804 | 0.0905 | 0.0871 |
| $V^{(c)}$ | 0.306 | 0.273 | 0.331 | 0.260 | 0.272 |

Comparison of the data presented in Tables 1 and 3 shows that the change of the ratio between the contents of particles of different fractions weakly affects the accuracy of determination of the total packing factor $V$. The situation is different if separating the fractions. In comparing, one should remember that, as $p$ increases from 0.2 to 0.5, the relative fraction of submicron particles significantly decreases in the volume content from 45 to 20%, though the essential increase of the total volume of particles (almost by 70%) occurs. So it is more correct to compare the retrieved partial factors $V^{(s)}$ and $V^{(c)}$ at different $p$ values related to the corresponding total $V$ values. Taking into account the aforesaid, for example, at the known value of the refractive index, the error in retrieving the volume packing factor $V^{(s)}$ related to $V$ is 4 to 5% for both cases. Deviation between analogous results obtained by retrieving the volume packing factors $V^{(c)}$ is about 3%.

**Table 4. Retrieved values of the mean radii of the model distributions in the problem of inverting the spectral dependences ε(λ) at $p = 0.5$ and $\delta = 0.1$**

| Parameter, μm | Exact data | $n = 1.5$ | $n = 1.45$ | $n = 1.55$ | $\kappa = 0.05$ |
|---|---|---|---|---|---|
| $\bar{r}_s$ | 0.725 | 0.737 | 0.768 | 0.660 | 0.650 |
| $\bar{r}_s^{(s)}$ | 0.258 | 0.315 | 0.276 | 0.269 | 0.259 |
| $\bar{r}_s^{(c)}$ | 1.317 | 1.367 | 1.356 | 1.334 | 1.258 |

Let us pass to the analysis of retrievals of the mean particle radius presented in Table 4 for the aerosol model with the parameter $p = 0.5$. First, let us note that the increase of $p$ leads to a shift of the mean radius $\bar{r}_s$ of the entire ensemble of particles to the right from 0.44 to 0.73 μm. Comparison of the data from Tables 2 and 4 shows that, as in the case of retrievals of the total packing factor $V$, the change of the ratio between the fractions practically does not affect the accuracy of determination of the mean radius $\bar{r}_s$ at the known refractive index. The absolute values of the errors in determining the mean radii of particles of s and c fraction $\bar{r}_s^{(s)}$ and $\bar{r}_s^{(c)}$ took close values of 0.05–0.06 μm. Taking into account uncertainties in setting the refractive index to be about 0.05, the maximum error in determining $\bar{r}_s$ does not exceed 0.075 μm.

## 3. Inversions of measured aureole scattering phase functions

One can conclude, based on the numerical simulation of solving the inverse problem for spectral measurements of extinction, that aforementioned measurements are quite sufficient for effective retrieval of both the aerosol size distribution function and the integral parameters of aerosol microstructure at wide variations of their disperse composition, especially at the known value of the refractive index of the particulate matter.

From the standpoint of obtaining data on the aerosol microphysical properties, it is interesting to compare two optical methods of diagnostics: using measurements of the spectral extinction of light and scattered light in the solar aureole.

As the inversion of aureole measurements of the scattering phase functions show, the accuracy of

retrievals is not high for submicron particles, where spectral measurements of the extinction of light have obvious advantages. The characteristics of accuracy of both methods are comparable for large particles. This result is quite predictable based on comparison of the scattering properties of coarse and submicron particles in the small-angle range shown in Fig. 3. In order to increase the role of submicron particles in the aureole range, it is necessary to perform angular measurements of the scattering phase functions in the UV wavelength range.

Angular dependences of the model scattering phase functions at three wavelength $\lambda = 0.31$, 0.4, and 0.55 μm are shown in Fig. 6. The dependences were chosen for solving the inverse problem at $p = 0.2$.

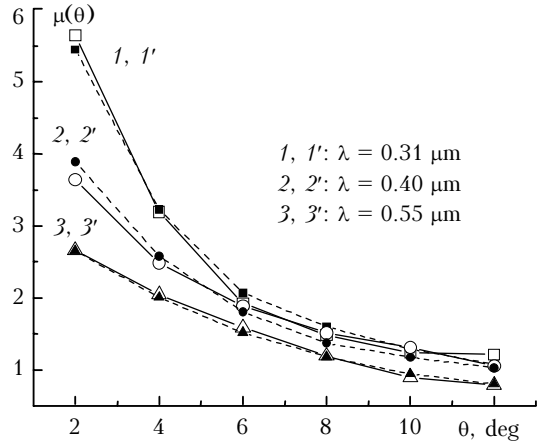


**Fig. 6.** Angular dependences of the scattering phase functions μ(θ) at three wavelengths. Solid curves have been calculated using the model distribution $S_{\downarrow 0}(r)$ at $p = 0.2$; dotted curves were calculated using the distribution retrieved from solution of the inverse problem for the scattering phase functions shown in Fig. 7 (curve *1*).

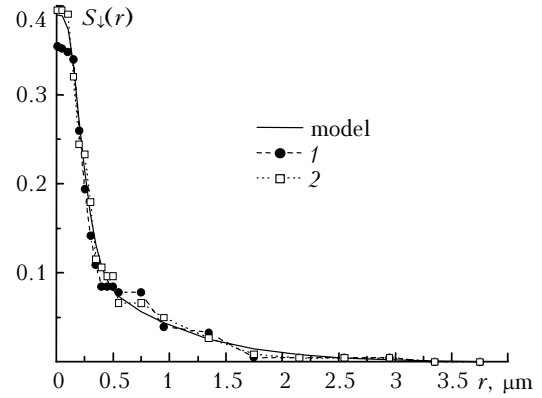


**Fig. 7.** Aerosol distributions $S_{\downarrow\delta}(r)$ retrieved by inverting the scattering phase function μ(θ) shown in Fig. 6 (curve *1*) and with the supplementary measurements of the extinction coefficient ε(λ) (curve *2*).

The random errors in measured scattering phase functions were simulated according to Eq. (1) at $\delta = 0.1$. The retrieved integral distribution $S_{\downarrow\delta}(r)$ is shown in Fig. 7 (curve *1*). The main difference of the presented solution from that obtained by the inversion of the spectral data on the extinction coefficient is, first, in the underestimation of the $S_{\downarrow\delta}(r)$ function at small radii, $r < 0.15$ μm, and, second, in more complete account of the coarse particles due to the shift of the upper boundary of the non-zero values of the retrieved distribution to the right up to 3.35 μm.

These peculiarities manifested themselves in the estimates of the parameters of microstructure presented in Tables 5 and 6.

**Table 5. Retrieved values of the volume packing factor *V* in the problem of inverting the aureole scattering phase function at $p = 0.2$ and $\delta = 0.1$**

| Parameter | Exact data | $n = 1.5$ | $n = 1.45$ | $n = 1.55$ | $\kappa = 0.05$ | $(\mu + \varepsilon)$ |
|---|---|---|---|---|---|---|
| $V$ | 0.227 | 0.217 | 0.204 | 0.223 | 0.241 | 0.227 |
| $V^{(s)}$ | 0.102 | 0.0865 | 0.0885 | 0.0926 | 0.132 | 0.108 |
| $V^{(c)}$ | 0.125 | 0.131 | 0.116 | 0.130 | 0.109 | 0.120 |

**Table 6. Retrieved values of the mean radii of the model distributions in the problem of inverting the aureole scattering phase function at $p = 0.2$ and $\delta = 0.1$**

| Parameter, μm | Exact data | $n = 1.5$ | $n = 1.45$ | $n = 1.55$ | $\kappa = 0.05$ | $(\mu + \varepsilon)$ |
|---|---|---|---|---|---|---|
| $\bar{r}_s$ | 0.437 | 0.459 | 0.559 | 0.465 | 0.467 | 0.431 |
| $\bar{r}_s^{(s)}$ | 0.241 | 0.235 | 0.317 | 0.253 | 0.301 | 0.245 |
| $\bar{r}_s^{(c)}$ | 1.285 | 1.253 | 1.335 | 1.148 | 1.388 | 1.357 |

It is seen from Table 5, that the error in determining the total packing factor $V$ in the considered example is about 4% at the known refractive index and does not exceed 10% at the errors in setting the refractive index $|\Delta n|$, $|\Delta\kappa| = 0.05$. These estimates, as well as the estimates of the mean radius $\bar{r}_s$ presented in Table 6, are close to the results obtained by inverting the spectral dependences of the extinction coefficient.

As to the estimation of analogous parameters of individual fractions, we have different situation. At high accuracy of estimation of the mean radius of s fraction $\bar{r}_s^{(s)}$ measurements of the aureole scattering phase functions of the ensemble of particles with the known refractive index provide for underestimated value of the volume packing factor $V^{(s)}$ with the error of 16%. The parameters of c fraction are retrieved more accurately. In particular, the errors in determining the volume packing factor $V^{(c)}$ at the known value of the refractive index decrease by about two times being of 5%, and the mean radius $\bar{r}_s^{(c)}$ can be determined with the error of 3%.

Finally, let us briefly consider the joint inversion of the spectral measurements of the extinction coefficient and the scattering phase function. The conditions of simulation corresponded to the aforementioned examples for each optical parameter at $p = 0.2$ and known value of the refractive index. The retrieved integral distribution $S_{\downarrow\delta}(r)$ is shown in Fig. 7 (curve *2*), and the relevant parameters of microstructure are presented in the last columns of Tables 5 and 6. Comparison of curves *1* and *2* in

Fig. 7 shows noticeable improvement of the retrievals of the $S_{\downarrow\delta}(r)$ function in the range of small radii $r$ if combining the spectral measurements of the extinction coefficient with the measurements of the scattering phase functions. Certain improvement of the accuracy of solution of the inverse problem is reached also in the entire size range.

In retrieving the integral parameters of particles, the difference in the obtained results is observed first of all in a more accurate determination of the volume content $V^{(s)}$ of the particles of s fraction relative to the results obtained by separately inverting the characteristics $\varepsilon(\lambda)$ and $\mu(\theta)$. As is seen in Table 5, measurements of $\mu(\theta)$ provide for high accuracy of estimation of the $V^{(c)}$ parameter of the coarse aerosol fraction. Additional data on light extinction does not affect the accuracy of the result obtained.

In retrieving the mean radius of particles $\bar{r}_s$ the error also has decreased, though in fact it was already quite low. On the contrary, use of additional measurements of $\varepsilon(\lambda)$ for estimation of the mean radius $\bar{r}_s^{(c)}$ of the coarse fraction leads to worsening the result, which has approached to the value obtained from measurements of the spectral extinction only.

## Conclusions

The vast information about estimation of the possibilities of applying the integral distributions to solving the inverse problems in sun photometry is obtained from the numerical experiments performed. The model of aerosol comprising the submicron and coarse aerosol fractions was used in calculations, the relative volume content of the submicron fraction changed from 20 to 100%.

It is shown that the technique developed for solving the inverse problem makes it possible to control the aerosol microstructure, including such its parameters as geometrical cross section, volume packing factor, mean radius in the wide size range, including separation of the fractions. No more than 1 to 2% of particles, by the total geometrical cross section, are left out of the size boundaries considered.

The parameters of microstructure are retrieved more accurate, which characterize the ensemble of particles as a whole. The error in retrieving the volume packing factor at the accuracy provided by sun photometers in real measurements of the atmospheric transmission and the known refractive index does not exceed 6% and increases up to 10% for individual fractions.

The mean radius of the entire ensemble of particles under the same conditions can be determined with the error of about 0.02 μm. This value for individual fractions reaches the level of 0.06 μm and can vary depending on their relative contribution to the measured characteristics.

As the numerical experiments show, angular measurements of the scattering phase functions in the aureole range of scattering angles have little information content on the properties of submicron aerosol and are comparable in the accuracy of retrieval of the parameters of microstructure with the spectral measurements of the transmission assuming wide aerosol distributions that involve the coarse fraction. In particular, one can retrieve the value of the packing factor of the coarse fraction from measurements of the aureole scattering phase functions with the error about 5%, and the mean radius with the error of 0.03 μm.

The greatest positive effect of the joint inversion of spectral measurements of the extinction coefficient and the aureole scattering phase functions is reached in a more accurate estimate of the volume content of particles of submicron fraction as compared to the results obtained at inverting these characteristics separately.

### Acknowledgments

The work was supported in part by the Russian Foundation for Basic Research (grant No. 05–05–64410).

### References

1. V.V. Veretennikov, Atmos. Oceanic Opt. **19**, No. 4, 259–265 (2006).
2. D. Deirmendjian, *Electromagnetic Scattering on Spherical Polydispersions* (Elsevier, New York, 1969).